Time-Delay Control of Quadrotor Unmanned Aerial Vehicles: A Multiplicity-Induced-Dominancy Based Approach

José de Jesus Castillo-Zamora, Islam Boussaada, Amina Benarab, Juan Escareno

Time-Delay Control of Quadrotor Unmanned Aerial Vehicles: A Multiplicity-Induced-Dominancy Based Approach

(To appear in: Journal of Vibration and Control)

José J. Castillo-Zamora[*], Islam Boussaada[*], Amina Benarab[*], Juan Escareno [†]

February 8, 2022

Abstract

The current work exploits the effects of time-delays on the stability of Unmanned Aerial Vehicles (UAVs). In this regard, the main contribution is a symbolic/numeric application of the Multiplicity-Induced-Dominancy (MID) property in the control of UAVs rotorcrafts featuring time-delays. The MID property is considered to address two of the most representative aerial robotic platforms: a classical quadrotor vehicle and a quadrotor vehicle endowed with tilting-rotors. The aforementioned property leads to an effective delayed feedback control design (MID tuning criteria), allowing the system to meet prescribed behavior conditions based on the placement of the rightmost root of the corresponding closed-loop characteristic function/quasipolynomial. Lastly, the results of detailed numerical simulations, including the linear and non-linear dynamics of the vehicle, are presented and discussed to validate the proposal.

Keywords. Multiplicity-Induced-Dominancy, Quadrotor, Time-Delay Control, Stability, Unmanned Aerial Vehicles.

1 Introduction

Among the actual technological surge, Unmanned Aerial Vehicles (UAVs) remain as a popular and challenging topic within the control systems and robotics scientific community. Such attractiveness relies on their friendly design and controllability criteria that

[*]Université Paris-Saclay, CNRS, CentraleSupélec, Inria, Laboratoire des signaux et systèmes, 91190, Gif-sur-Yvette, France. Institut Polytechnique des Sciences Avancées (IPSA). 63 boulevard de Brandebourg, 94200 Ivry-sur-Seine, France. E-mails: {first name.last name}@l2s.centralesupelec.fr

[†]ENSIL-ENSCI, Limoges, CNRS, XLIM, UMR, France

have led to a wide application range such as high-precision weather monitoring, precision agriculture, swarm-based distributed perception, among others [13, 50, 54].
The capability of UAVs to perform accurate maneuvers is strongly dependent on the efficient synthesis and implementation of control-task-oriented algorithms. Several of these strategies take into consideration quaternion-based modeling approaches [2], image-aimed stabilization, or the well-known proportional-derivative (PD) and proportional-integral-derivative (PID) controllers [15, 16, 59]. In addition, robust control techniques [18, 29] and state observers [14, 17, 18, 21] have been also been used.
Among the variety of issues undermining the aerial systems performance, the study of time-delay effects remains relatively unexplored. In practice, UAVs' control systems operate in presence of time-delays arising from perception processing, decision-making, control commands and actuators' delayed dynamics. It has been proved that time-delays induce oscillatory phenomena rendering the system unstable. Nevertheless, some stabilizing effects of time-delays can be exploited to improve the system's performance [48, 57].
The stability of aerial vehicles under the influence of time-delays has been addressed in works as [19,39] which provide a set of parametric stability charts. Meanwhile, [36] considers the full non-linear dynamics to study the trajectory tracking problem. It is worthwhile highlighting that a considerable amount of prior works focuses on the communication and information exchange processes as the main sources of time-delays [3, 31, 46, 55]. In this regard, the range of solutions to overcome such an issue goes from delay-optimization approaches [35] to Backstepping and non-linear control [20, 30, 38] yet, a vast variety of different approaches can be found in the literature, see for instance [25, 43–45, 48, 60].
Amidst the novel techniques regarding time-delay systems analysis, tracking the behavior of the roots of the characteristic equation, as in [8], has led to an increasing interest on exploiting the Multiplicity-Induced-Dominancy (MID) property which refers to a special condition where a given root of the characteristic function matches the spectral abscissa such that the corresponding spectral value is dominant.
The MID property has already been suggested to solve some low-order cases [27] and some other phenomena described by linear time-delay differential equations [7, 9–11, 41]. Recent results in this direction provide necessary and sufficient conditions for roots of maximal multiplicity in reduced-order time-delay systems of retarded [10, 41] and neutral types [6, 40]. Nevertheless, the application of such findings on the domain of aerial robots control, as far as it is concerned to the authors, has not been specifically considered.
The current investigation exploits the effects of the time-delay, due to the latency of generic indoor-positioning systems, to stabilize two popular rotorcrafts: (i) a classical "+" quadrotor and (ii) a "+" quadrotor endowing 1-Degree-Of-Freedom (DOF) tilting-rotors. The MID property defines a tuning criteria of the controllers' gains such that a non-oscillatory transient response of the vehicle obeys a prescribed decay rate.
The sequel of the manuscript is outlined in the following manner: Section 2 provides a brief introduction to time-delay differential equations and the MID property fundamentals. In Section 3, the dynamics of the quadrotor vehicles is described. Section 4 is devoted to the conception of the controllers that stabilize the typical quadrotor vehicle. On the other hand, Section 5 exposes the control strategy adopted to stabilize the UAV endowed with 1-DOF tilting-rotors. Section 6 provides the results of the detailed numerical simulations carried out to validate the proposals. Lastly, concluding remarks are given in Section 7.

2 Fundamentals of the MID Property and Time-Delay Differential Equations

The MID property refers to conditions under which multiple roots of the characteristic function match the spectral abscissa. Some recent works have shown that a spectral value of maximal multiplicity of a time-delay system is necessarily real and corresponds to the spectral abscissa, a property called *generic multiplicity-induced-dominancy*, or GMID for short, see for instance [6, 42]. However, in the case of a root of strictly intermediate multiplicity, one has to seek for conditions on the system's free parameters (typically the control parameters) for the MID to hold. These conditions allow to define the admissible assignment region, see for instance [4, 5, 10].
An extensive literature, regarding the analysis of linear time-delay systems described by retarded delay differential equations of the form:

$$\mathcal{F}^{(n)}(t) + a_{n-1}\mathcal{F}^{(n-1)}(t) + \ldots + a_0\mathcal{F}(t) + \varphi_{n-1}\mathcal{F}^{(n-1)}(t-\tau) + \ldots + \varphi_0\mathcal{F}(t-\tau) = 0 \tag{2.1}$$

is available (see for instance [43]). In such a system representation, $\mathcal{F}$ is an unknown real-valued function, n is a positive integer, $a_k, \varphi_k \in \mathbb{R}$ for $k \in \{0, ..., n-1\}$ are constant coefficients, and $\tau > 0$ is a time-delay.
The analysis of (2.1) occurs to be important as it represents linear control systems subjected a control input and a time-delay feedback $u(t-\tau)$, such that:

$$\mathcal{F}^{(n)}(t) + a_{(n-1)}\mathcal{F}^{n-1}(t) + \ldots + a_0\mathcal{F}(t) = u(t-\tau) \tag{2.2}$$

In the time-delay-free scenario, the control input is often established as the following $u(t) = -\varphi_{n-1}\mathcal{F}^{(n-1)}(t) - \ldots - \varphi_0\mathcal{F}(t)$, assuming that the measurement of $\mathcal{F}(t)$ and its derivatives $\mathcal{F}^{(n-1)}(t), \ldots, \mathcal{F}'(t)$ are instantaneously available; thus the roots of the characteristic function can be strategically chosen, according to a desired exponential behavior, by a proper selection of the coefficients $\varphi_0, \ldots, \varphi_{n-1}$. For some additional insights, a further conceptualization and illustrative examples on this matter, one may refer, but may not limit, to [22, 53].
Spectral methods are equally adopted to address systems with time-delays. In this regard, the asymptotic behavior of the solutions depends on the roots of the characteristic function which, for (2.1), is defined as $\Delta : \mathbb{C} \to \mathbb{C}$ for $s \in \mathbb{C}$ such that:

$$\Delta(s) = s^n + \sum_{k=0}^{n-1} a_k s^k + e^{-s\tau} \sum_{k=0}^{n-1} \varphi_k s^k \tag{2.3}$$

Thus $\sigma_0 = \sup\{\mathrm{Re}\{s\} | s \in \mathbb{C}, \Delta(s) = 0\}$ defines the exponential behavior of the solutions of (2.1). The real number σ_0 is named the spectral abscissa of Δ and it follows that for every $\epsilon > 0$, there exists a $\kappa < 0$ such that for every solution $\mathcal{F}$ of (2.1), one has $|\mathcal{F}(t)| \leq \kappa e^{(\sigma_0+\epsilon)t} \max_{\vartheta \in [-\tau, 0]} |\mathcal{F}(\vartheta)|$ [26]. In addition, to ensure the exponential convergence of the solutions to 0, $\sigma < 0$ shall strictly hold. Nevertheless, the analysis of the (asymptotic) behavior of the solution of (2.1) stands as a challenge since the corresponding characteristic function Δ has infinitely many roots.
If Δ possesses a dominant root with negative real part, then the exponential stability of (2.1) is equivalent to it. Additionally, it may hold, for some characteristic quasipolynomials of time-delay systems, that the real roots of maximal multiplicity are dominant which gives

name to the Multiplicity-Induced-Dominancy (MID) property. Thus, it follows that a root s_0 with multiplicity $n \in \mathbb{N}$ satisfies:

$$\Delta(s_0) = \Delta'(s_0) = \ldots = \Delta^{(n-2)}(s_0) = \Delta^{(n-1)}(s_0) = 0 \tag{2.4}$$

The formal definition of a *quasipolynomial* is provided below.

Definition 2.1. A quasipolynomial Λ is an entire function $\Lambda : \mathbb{C} \to \mathbb{C}$ which can be written under the form

$$\Lambda(s) = \sum_{k=0}^{\iota} \varrho_k(s) e^{\lambda_k s} \tag{2.5}$$

where ι is a nonnegative integer, $\lambda_0, \ldots, \lambda_\iota$ are pairwise distinct real numbers, and, for $k \in \{0, \ldots, \iota\}$, ϱ_k is a nonzero polynomial with complex coefficients of degree $\mu_k \geq 0$. The integer $D = \iota + \sum_{k=0}^{\iota} \mu_k$ is called the degree of Λ. When $\lambda_0 = 0$ and $\lambda_k < 0$ for $k \in \{1, \ldots, \iota\}$ in (2.5), Λ is the characteristic function of a linear time-delay system with delays $-\lambda_1, \ldots, -\lambda_\iota$.

A set of necessary results and additional on quasipolynomials for the understanding and analysis of these, are given next:

- The roots of a quasipolynomial do not change when its coefficients are all multiplied by the same nonzero number, and hence one may always assume, without loss of generality, that one nonzero coefficient of a quasipolynomial is normalized to 1, such as the coefficient of the term of highest degree in ϱ_0.
- Let Λ be a quasipolynomial of degree D in the form of (2.5). Then any root $s_0 \in \mathbb{C}$ of Λ has multiplicity at most D.
- Let $\Lambda : \mathbb{C} \to \mathbb{C}$ and $s_0 \in \mathbb{C}$ be such that $\Lambda(s_0) = 0$. It is said that s_0 is a dominant (respectively, strictly dominant) root of Λ if, for every $s \in \mathbb{C} \backslash \{s_0\}$ such that $\Lambda(s) = 0$, one has $\mathrm{Re}\{s\} \leq \mathrm{Re}\{s_0\}$ (respectively, $\mathrm{Re}\{s\} < \mathrm{Re}\{s_0\}$).
- The roots of the quasipolynomial Δ in (2.3) with maximal multiplicity are necessarily dominant and such multiplicity can be attained only in the real axis.

For an extended and detailed treatment of these concerns, the reader is referred to [4, 5, 9, 10, 42, 45].

3 Quadrotor Model

Let the quadrotor system be depicted in Fig. 3.1. The vision-based tracking system permits to know the position of the vehicle, $\boldsymbol{\xi} = [x\ y\ z]^T \in \mathbb{R}^3$, in a conditioned environment. Such sensing strategy often takes a fraction of time $\tau > 0$ to be executed; this issue is translated to control terms as a feedback time-delay [28, 56].
The dynamics of the vehicle is described w.r.t. an inertial frame $O_I \{x_I, y_I, z_I\}$ and a body frame $O_b \{x_b, y_b, z_b\}$ whose origin matches the center of gravity (CoG) of the UAV. x_b, y_b, z_b define the roll, pitch and yaw axes and the corresponding principal axis of inertia which are associated to the Euler angles $\boldsymbol{\eta} = [\phi\ \theta\ \psi]^T \in \mathbb{R}^3$, respectively. The motion of the aerial vehicle can be described, according to the Newton Euler formulation [15, 16], as:

$$m_r \ddot{\boldsymbol{\xi}} + m_r \mathbf{g} = \boldsymbol{\tau}_{\boldsymbol{\xi}} \tag{3.1}$$

$$I\dot{\boldsymbol{\omega}} + \boldsymbol{\omega} \times (I\boldsymbol{\omega}) = \boldsymbol{\tau}_{\boldsymbol{\omega}} \tag{3.2}$$

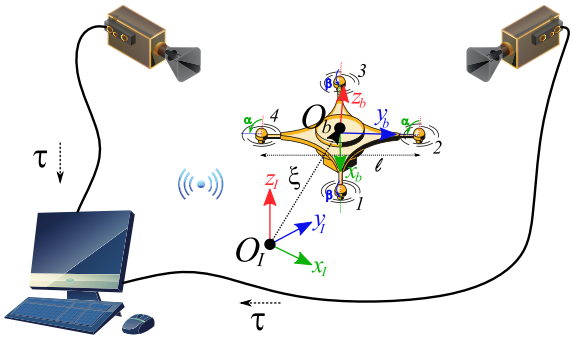

Figure 3.1: Quadrotor vehicle and vision-based tracking system (scheme conceived from figures available at *freepik.com*)

where $m_r > 0$ stands for the mass of the UAV and $\mathbf{g} = [0\ 0\ g]^T \in \mathbb{R}^3$ does for the vector containing the constant of gravity acceleration $g > 0$. $I = \text{diag}([I_x\ I_y\ I_z]^T) \in \mathbb{R}^{3\times 3}$ is respectively defined by the moments of inertia about the roll, pitch and yaw axis. For a given $\boldsymbol{\nu} \in \mathbb{R}^n$, the function $\text{diag} : \mathbb{R}^n \to \mathbb{R}^{n\times n}$ is defined by

$$\text{diag}(\boldsymbol{\nu}) = \begin{bmatrix} \nu_1 & 0 & \dots & 0 \\ 0 & \nu_2 & \dots & 0 \\ \vdots & \vdots & \ddots & \dots \\ 0 & 0 & \dots & \nu_n \end{bmatrix} \tag{3.3}$$

The angular velocity vector $\boldsymbol{\omega} = [p\ q\ r]^T \in \mathbb{R}^3$ is related to the Euler rates $\dot{\boldsymbol{\eta}}$ as follows

$$\boldsymbol{\omega} = W_{\boldsymbol{\eta}}\dot{\boldsymbol{\eta}} \quad \text{and} \quad W_{\boldsymbol{\eta}} = \begin{bmatrix} 1 & 0 & -\text{S}_\theta \\ 0 & \text{C}_\phi & \text{S}_\phi\text{C}_\theta \\ 0 & -\text{S}_\phi & \text{C}_\phi\text{C}_\theta \end{bmatrix} \in \mathbb{R}^{3\times 3} \tag{3.4}$$

where $\text{C}_{(\bullet)} = \cos(\bullet)$ and $\text{S}_{(\bullet)} = \sin(\bullet)$. Such an abuse of this notation is considered throughout the sequel of the manuscript.
The translational motion described by (3.1) is provided in terms of the inertial frame. On the other hand, (3.2) describes the rotational motion of the quadrotor in the body reference frame.
The actuation of the system stands as the main difference between a typical quadrotor and a quadrotor endowed with tilting-rotors. In this sense, the translational motion of the aircraft is driven by the forces comprised in the vector $\boldsymbol{\tau}_{\boldsymbol{\xi}} \in \mathbb{R}^3$ which is defined, for the typical quadrotor, by the rotation matrix $R_{\boldsymbol{\eta}} \in \mathbb{R}^{3\times 3}$ and the forces of the propellers $f_i \geq 0$ (with $i = 1, 2, 3, 4$), as:

$$\boldsymbol{\tau}_{\boldsymbol{\xi}} = R_{\boldsymbol{\eta}} \begin{bmatrix} 0 \\ 0 \\ T = f_1 + f_2 + f_3 + f_4 \end{bmatrix} \quad \text{and} \quad R_{\boldsymbol{\eta}} = \begin{bmatrix} \text{C}_\theta\text{C}_\psi & \text{S}_\phi\text{S}_\theta\text{C}_\psi - \text{C}_\phi\text{S}_\psi & \text{C}_\phi\text{S}_\theta\text{C}_\psi + \text{S}_\phi\text{S}_\psi \\ \text{C}_\theta\text{S}_\psi & \text{S}_\phi\text{S}_\theta\text{S}_\psi + \text{C}_\phi\text{C}_\psi & \text{C}_\phi\text{S}_\theta\text{S}_\psi - \text{S}_\phi\text{C}_\psi \\ -\text{S}_\theta & \text{S}_\phi\text{C}_\theta & \text{C}_\phi\text{C}_\theta \end{bmatrix} \tag{3.5}$$

For the quadrotor endowed with 1-DOF tilting-rotors, the vector $\boldsymbol{\tau}_{\boldsymbol{\xi}}$ is rewritten in terms of $R_{\boldsymbol{\eta}}$, f_i and the tilt angles α and $\beta \in \mathbb{R}$ as:

$$\boldsymbol{\tau}_{\boldsymbol{\xi}} = R_{\boldsymbol{\eta}} \begin{bmatrix} (f_1 + f_3)\,\text{S}_\beta \\ -(f_2 + f_4)\,\text{S}_\alpha \\ (f_1 + f_3)\,\text{C}_\beta + (f_2 + f_4)\,\text{C}_\alpha \end{bmatrix} \tag{3.6}$$

The rotational states of the aircraft are controlled by the torques in the vector $\boldsymbol{\tau_\omega} \in \mathbb{R}^3$ which, for the typical quadrotor structure, is defined as:

$$\boldsymbol{\tau_\omega} = \begin{bmatrix} \tau_\phi = \ell\,(f_2 - f_4)\,/2 \\ \tau_\theta = \ell\,(f_3 - f_1)\,/2 \\ \tau_\psi = \varepsilon\,(f_1 - f_2 + f_3 - f_4) \end{bmatrix} \tag{3.7}$$

where $\ell > 0$ denotes the diagonal motor-to-motor distance and $\varepsilon > 0$ is a proportionality constant that relates the force f_i to the corresponding free moment τ_i such that $\tau_i = \varepsilon f_i$. For the quadrotor vehicle equipped with tilting-rotors, $\boldsymbol{\tau_\omega}$ reads as:

$$\boldsymbol{\tau_\omega} = \begin{bmatrix} \ell\,(f_2 - f_4)\,\mathrm{C}_\alpha/2 + \varepsilon\,(f_1 + f_3)\,\mathrm{S}_\beta \\ \ell\,(f_3 - f_1)\,\mathrm{C}_\beta/2 - \varepsilon\,(f_2 + f_4)\,\mathrm{S}_\alpha \\ \varepsilon\,[(f_1 + f_3)\,\mathrm{C}_\beta - (f_2 + f_4)\,\mathrm{C}_\alpha] \end{bmatrix} \tag{3.8}$$

This non-linear description of the vehicles dynamics allows one to proceed to the conception of the controllers.

4 UAV Control: The Typical Quadrotor Case

Let the typical quadrotor vehicle be firstly addressed. As it can be found in the literature [15, 19, 28, 39], it is typically assumed that the vehicle operates at low speeds in a quasi-hover state ($\phi, \theta \approx 0$ and, without loss of generality, $\psi = 0$), such that the Coriolis and Centripetal effects are neglected. These considerations lead to a linear representation of (3.1), (3.2), (3.5) and (3.7) of the form:

$$\begin{cases} X(s) = \dfrac{1}{m_r s^2}\theta(s)T(s), \quad Y(s) = -\dfrac{1}{m_r s^2}\phi(s)T(s), \quad Z(s) = \dfrac{1}{m_r s^2}\left(T(s) - m_r g\right), \\ \phi(s) = \dfrac{1}{I_x s^2}\tau_\phi(s), \quad \theta(s) = \dfrac{1}{I_y s^2}\tau_\theta(s), \quad \psi(s) = \dfrac{1}{I_z s^2}\tau_\psi(s) \end{cases} \tag{4.1}$$

which corresponds to a description of the system in the frequency domain where $s = \sigma + j\omega$ with $\sigma, \omega \in \mathbb{R}$.
From (4.1), it is immediate to observe that the $Z(s)$ and $\psi(s)$ motions are decoupled, yet the $X(s)$ dynamics is coupled to that of $\theta(s)$ and the $Y(s)$ motion is related to that of $\phi(s)$. In this regard, let the thrust $T(s)$ be used as the control input to drive the system to a desired height $Z_d(s)$ and $\tau_\psi(s)$ does the proper to keep the yaw angle at 0. These control inputs are respectively defined, as:

$$T(s) = m_r\left(\mathcal{C}_z(s)\,E_z(s) + g\right) \quad \text{and} \quad \tau_\psi(s) = I_z\mathcal{C}_\psi(s)\,E_\psi(s) \tag{4.2}$$

where the z error reads as $E_z(s) = Z_d(s) - e^{-\tau s}Z(s)$ since the translational states of the quadrotor are subjected to a feedback time-delay τ due to the inherent latency of the vision-based tracking system, and the ψ error stands as $E_\psi(s) = -\psi(s)$ since $\psi_d(s) = 0$. The linear controllers $\mathcal{C}_z(s)$ and $\mathcal{C}_\psi(s)$ correspond to PD controllers of the form:

$$\mathcal{C}_z(s) = k_{p_z} + k_{d_z}s \quad \text{and} \quad \mathcal{C}_\psi(s) = k_{p_\psi} + k_{d_\psi}s \tag{4.3}$$

with $k_{p_z}, k_{p_\psi} \in \mathbb{R}$ defined as the proportional gains and $k_{d_z}, k_{d_\psi} \in \mathbb{R}$ standing as the derivative gains. The aforementioned control gains are tuned, as exposed in the sequel of the manuscript, by means of the MID property since a time-delay affects the corresponding

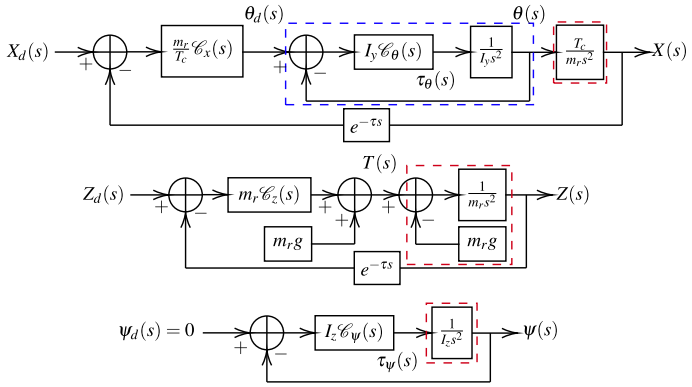

Figure 4.1: Block diagram representation of the typical quadrotor closed-loop system

dynamics.
Regarding the translational motion of the vehicle, let one consider that, for a large enough time, $T(s) \to T_c = m_r g$ as $Z(s) \to Z_d(s)$ [39, 58]. The latter allows one to rewrite the equations of motion for $X(s)$ and $Y(s)$ in (4.1) as:

$$X(s) = \frac{1}{m_r s^2}\theta(s)T_c \quad \text{and} \quad Y(s) = -\frac{1}{m_r s^2}\phi(s)T_c \tag{4.4}$$

It is thus considered that $\theta(s)$ and $\phi(s)$ act as the control inputs for the corresponding DOF, such that the reference values are defined by linear PD controllers, $\mathcal{C}_x(s)$ and $\mathcal{C}_y(s)$, as follows

$$\theta_d(s) = \frac{m_r}{T_c}\mathcal{C}_x(s)E_x(s) \quad \text{and} \quad \phi_d(s) = -\frac{m_r}{T_c}\mathcal{C}_y(s)E_y(s) \tag{4.5}$$

with

$$\mathcal{C}_x(s) = k_{p_x} + k_{d_x}s, \quad \mathcal{C}_y(s) = k_{p_y} + k_{d_y}s \tag{4.6}$$

$$E_x(s) = X_d(s) - e^{-\tau s}X(s), \quad E_y(s) = Y_d(s) - e^{-\tau s}Y(s) \tag{4.7}$$

where the proportional gains correspond to $k_{p_x}, k_{p_y} \in \mathbb{R}$, and the derivative gains are denoted by $k_{d_x}, k_{d_y} \in \mathbb{R}$. Moreover, the reference values in (4.5) are achieved by the action of the linear PD controllers:

$$\mathcal{C}_\theta(s) = k_{p_\theta} + k_{d_\theta}s \quad \text{and} \quad \mathcal{C}_\phi(s) = k_{p_\phi} + k_{d_\phi}s \tag{4.8}$$

such that:

$$\tau_\theta(s) = I_y\mathcal{C}_\theta(s)E_\theta(s) \quad \text{and} \quad \tau_\phi(s) = I_x\mathcal{C}_\phi(s)E_\phi(s) \tag{4.9}$$

with $E_\theta(s) = \theta_d(s) - \theta(s)$ and $E_\phi(s) = \phi_d(s) - \phi(s)$. The proportional gains $k_{p_\theta}, k_{p_\phi} \in \mathbb{R}$ as well as the derivative gains $k_{d_\theta}, k_{d_\phi} \in \mathbb{R}$ are tuned in such a manner that the rotational dynamics is stable and faster than that of translation [58].
To synthesize the previous establishments, the $X(s)$, $Z(s)$ and $\psi(s)$ closed-loop systems are depicted in Fig. 4.1 where the dynamics of the plant is highlighted in red and the inner dynamics is surrounded by a black dashed box. Notice that the $Y(s)$ dynamics is omitted since it follows the same structure as that of $X(s)$.

4.1 MID-Property-Based Controllers Analysis

According to Fig. 4.1, the closed-loop transfer functions of each DOF can be computed such that the characteristic functions correspond to:

$$\Delta_x(s) = s^2\left[s^2 + \mathcal{C}_\theta(s)\right] + e^{-\tau s}\mathcal{C}_x(s)\mathcal{C}_\theta(s) \tag{4.10}$$

$$\Delta_y(s) = s^2\left[s^2 + \mathcal{C}_\phi(s)\right] + e^{-\tau s}\mathcal{C}_y(s)\mathcal{C}_\phi(s) \tag{4.11}$$

$$\Delta_z(s) = s^2 + e^{-\tau s}\mathcal{C}_z(s) \tag{4.12}$$

$$\Delta_\psi(s) = s^2 + \mathcal{C}_\psi(s) \tag{4.13}$$

Regarding (4.13), no time-delay effect is present thus, the exponential behavior of the solutions can be tuned by the proper placement of the roots of the polynomial. In this sense, it is enough that such roots rely on the left-plane of the complex space, moreover, a non-oscillatory stable system's response is achieved if the roots are real, see for instance [58]. The latter is comprised in Proposition 4.1 below.

Proposition 4.1. *For the closed-loop dynamics described by (4.13), a non-oscillatory stable system's response is achieved and guaranteed if the controller's gains satisfy:*

$$k_{d_\psi} = s_{\psi,1} + s_{\psi,2} \quad \textit{and} \quad k_{p_\psi} = s_{\psi,1}s_{\psi,2} \tag{4.14}$$

with $s_{\psi,2} > s_{\psi,1} > 0$.

Proof. The proof is provided by the substitution of the gains given in (4.14) into (4.13) leading to:

$$s^2 + (s_{\psi,1} + s_{\psi,2})\,s + s_{\psi,1}s_{\psi,2} = (s + s_{\psi,1})\,(s + s_{\psi,2}) = 0 \tag{4.15}$$

such that the roots of the system are located at $s = -s_{\psi,1}$ and $s = -s_{\psi,2}$.

□

It must be noticed that Proposition 4.1 can be applied to stabilize the inner-loop dynamics highlighted in black in Fig. 4.1 as the existence of negative real roots of the characteristic function of the open-loop system is essential to exploit the MID property. Regarding the translational dynamics where the time-delay effect is found, the analysis of the $Z(s)$ dynamics is provided at first place, afterwards, the $X(s)$ dynamics of the vehicle is studied.
The following result, which is a direct consequence of [10], permits to characterize an assignable spectral value guaranteeing $\sigma-$stability as well as the corresponding controller's gains.

Proposition 4.2. *For the quasipolynomial in (4.12), the following assertions hold:*

(a) *The multiplicity of any given root of the quasipolynomial function is bounded by 4.*

(b) *For a positive delay* τ*, the quasipolynomial in (4.12) admits a real spectral value at* $s = s_{0_z}$ *with algebraic multiplicity 3 if and only if:*

$$s_{0_z} = \frac{-2 + \sqrt{2}}{\tau} \tag{4.16}$$

and the controller's gains satisfy:

$$k_{p_z} = e^{\tau s_{0_z}} s_{0_z}^2\,(s_{0_z}\tau + 1) \quad \textit{and} \quad k_{d_z} = -e^{\tau s_{0_z}}\,s_{0_z}\,(s_{0_z}\tau + 2) \tag{4.17}$$

Proof. The first statement of the proposition is a direct assimilation of the results presented at [9]. On the other hand, if s_{0_z} is a root with multiplicity at least 2, it follows that: $\Delta_z(s_{0_z}) = \Delta_z'(s_{0_z}) = 0$. By solving these equations for the control gains, the in (4.17) are obtained. The root s_{0_z} reaches a multiplicity 3 if and only if:

$$\Delta_z''(s_{0_z}) = 2 + e^{-\tau s_{0_z}} \left[\tau^2 \left(k_{d_z} s_{0_z} + k_{p_z}\right) - 2\tau k_{d_z}\right] = 0 \tag{4.18}$$

The substitution of (4.17) into (4.18) leads to (4.16). To prove that s_{0_z} is the dominant root, one may exploit the result from [10, Theorem 4.2].

□

Let one proceed to study the quasipolynomial in (4.10). In this regard, and due to the complexity of the expressions, a useful proposition based on a symbolic/numerical analysis is provided next.

4.2 Symbolic/Numeric Analysis of the MID-Based Controller

Firstly, to study the behavior of the system whose characteristic function corresponds to the quasipolynomial provided in (4.10), one must ensure that the delay-free part of the quasipolynomial has only real roots which occurs if:

$$k_{d_\theta}^2 > 4k_{p_\theta} > 0 \tag{4.19}$$

which is equivalent to Proposition (4.1). This condition over the gains k_{p_θ} and k_{d_θ} is taken into consideration to exploit the MID property as numerically/symbolically established next.

Proposition 4.3. *For the quasipolynomial in (4.10), the following assertions hold:*

(a) *The multiplicity of any given root of the quasipolynomial function is bounded by 7.*

(b) *For a given positive delay τ, an arbitrary root s_{0_x} with algebraic multiplicity 4 is a dominant root of (4.10) if $s_{0_x} \in \mathbb{B}$, where*

$$\mathbb{B} = \left\{ s_{0_x} : -\frac{3}{10\,\tau} < s_{0_x} < 0 \right\} \tag{4.20}$$

and the controllers' gains k_{p_θ}, k_{d_θ}, k_{p_x} and k_{d_x} satisfy:

$$k_{p_\theta} = \lambda s_{0_x}^2, \quad k_{d_\theta} = -\frac{s_{0_x}}{9}\left(\frac{n_2\lambda^2 - n_1\lambda + n_0}{d_2\lambda^2 - d_1\lambda + d_0}\right) \tag{4.21}$$

$$k_{p_x} = \frac{s_{0_x}^2 e^{\tau s_{0_x}}}{\mathcal{C}_\theta^2\left(s_{0_x}\right)}\left\{\mathcal{C}_\theta\left(s_{0_x}\right)\left(\tau s_{0_x} + 1\right)\left[s_{0_x}^2 + \mathcal{C}_\theta\left(s_{0_x}\right)\right] + s_{0_x}^2\left[\mathcal{C}_\theta\left(s_{0_x}\right) + k_{p_\theta}\right]\right\} \tag{4.22}$$

$$k_{d_x} = \frac{-s_{0_x} e^{\tau s_{0_x}}}{\mathcal{C}_\theta^2\left(s_{0_x}\right)}\left\{\mathcal{C}_\theta\left(s_{0_x}\right)\left(\tau s_{0_x} + 2\right)\left[s_{0_x}^2 + \mathcal{C}_\theta\left(s_{0_x}\right)\right] + s_{0_x}^2\left[\mathcal{C}_\theta\left(s_{0_x}\right) + k_{p_\theta}\right]\right\} \tag{4.23}$$

where λ is defined as the only positive real root of the following algebraic equation

$$p_3\lambda^3 + p_2\lambda^2 + p_1\lambda + p_0 = 0 \tag{4.24}$$

with

$$p_3 = 27\left(s_{0_x}^2\tau^2 + 4s_{0_x}\tau + 2\right)^4 \tag{4.25}$$

$$p_2 = -10s_{0_x}^9\tau^9 - 243s_{0_x}^8\tau^8 - 2352s_{0_x}^7\tau^7 - 12090s_{0_x}^6\tau^6 - 36360s_{0_x}^5\tau^5 - 65916s_{0_x}^4\tau^4 - 72288s_{0_x}^3\tau^3 - 47736s_{0_x}^2\tau^2 - 17280s_{0_x}\tau - 2592 \tag{4.26}$$

$$p_1 = \left(s_{0_x}^3\tau^3 + 12s_{0_x}^2\tau^2 + 36s_{0_x}\tau + 24\right)\left(s_{0_x}^3\tau^3 + 18s_{0_x}^2\tau^2 + 54s_{0_x}\tau + 24\right)\left(s_{0_x}^4\tau^4 + 8s_{0_x}^3\tau^3 + 24s_{0_x}^2\tau^2 + 24s_{0_x}\tau + 12\right) \tag{4.27}$$

$$p_0 = -\left(s_{0_x}^4\tau^4 + 8s_{0_x}^3\tau^3 + 24s_{0_x}^2\tau^2 + 24s_{0_x}\tau + 12\right)\left(s_{0_x}^3\tau^3 + 12s_{0_x}^2\tau^2 + 36s_{0_x}\tau + 24\right)^2 \tag{4.28}$$

and

$$n_2 = 11s_{0_x}^{12}\tau^{12} + 309s_{0_x}^{11}\tau^{11} + 3738s_{0_x}^{10}\tau^{10} + 25938s_{0_x}^9\tau^9 + 115452s_{0_x}^8\tau^8 + 348192s_{0_x}^7\tau^7 + 731016s_{0_x}^6\tau^6 + 1077408s_{0_x}^5\tau^5 + 1105920s_{0_x}^4\tau^4 + 771120s_{0_x}^3\tau^3 + 347328s_{0_x}^2\tau^2 + 90720s_{0_x}\tau + 10368 \tag{4.29}$$

$$n_1 = \left(s_{0_x}^3\tau^3 + 12s_{0_x}^2\tau^2 + 36s_{0_x}\tau + 24\right)\left(2s_{0_x}^6\tau^6 + 39s_{0_x}^5\tau^5 + 249s_{0_x}^4\tau^4 + 744s_{0_x}^3\tau^3 + 1116s_{0_x}^2\tau^2 + 756s_{0_x}\tau + 180\right)\left(s_{0_x}^4\tau^4 + 8s_{0_x}^3\tau^3 + 24s_{0_x}^2\tau^2 + 24s_{0_x}\tau + 12\right) \tag{4.30}$$

$$n_0 = 2\left(s_{0_x}^3\tau^3 + 6s_{0_x}^2\tau^2 + 12s_{0_x}\tau + 6\right)\left(s_{0_x}^4\tau^4 + 8s_{0_x}^3\tau^3 + 24s_{0_x}^2\tau^2 + 24s_{0_x}\tau + 12\right)\left(s_{0_x}^3\tau^3 + 12s_{0_x}^2\tau^2 + 36s_{0_x}\tau + 24\right)^2 \tag{4.31}$$

$$d_2 = 3\left(2s_{0_x}^3\tau^3 + 9s_{0_x}^2\tau^2 + 12s_{0_x}\tau + 6\right)\left(s_{0_x}^2\tau^2 + 4s_{0_x}\tau + 2\right)^4 \tag{4.32}$$

$$d_1 = (s_{0_x}^4\tau^4 + 16s_{0_x}^3\tau^3 + 63s_{0_x}^2\tau^2 + 84s_{0_x}\tau + 30)(s_{0_x}^4\tau^4 + 8s_{0_x}^3\tau^3 + 24s_{0_x}^2\tau^2 + 24s_{0_x}\tau + 12)(s_{0_x}^2\tau^2 + 4s_{0_x}\tau + 2)^2 \tag{4.33}$$

$$d_0 = (s_{0_x}\tau + 2)(s_{0_x}^3\tau^3 + 12s_{0_x}^2\tau^2 + 36s_{0_x}\tau + 24)(s_{0_x}^4\tau^4 + 8s_{0_x}^3\tau^3 + 24s_{0_x}^2\tau^2 + 24s_{0_x}\tau + 12)(s_{0_x}^2\tau^2 + 4s_{0_x}\tau + 2)^2 \tag{4.34}$$

Proof. The first statement of the proposition is a direct assimilation of the results presented at [9], see also [42]. Furthermore, (4.21)-(4.23) are found as in Proposition 4.2. In this regard, if s_{0_x} is a root with multiplicity at least 2, it follows that:

$$\Delta_x(s_{0_x}) = s_{0_x}^2\left(s_{0_x}^2 + k_{d_\theta}s_{0_x} + k_{p_\theta}\right) + e^{-\tau s_{0_x}}\left(k_{d_x}s_{0_x} + k_{p_x}\right)\left(k_{d_\theta}s_{0_x} + k_{p_\theta}\right) = 0 \tag{4.35}$$

$$\Delta_x'(s_{0_x}) = s_{0_x}\left(4s_{0_x}^2 + 3k_{d_\theta}s_{0_x} + 2k_{p_\theta}\right) - e^{-\tau s_{0_x}}\left[\tau\left(k_{d_x}s_{0_x} + k_{p_x}\right)\left(k_{d_\theta}s_{0_x} + k_{p_\theta}\right) - \left(2k_{d_\theta}k_{d_x}s_{0_x} + k_{p_x}k_{d_\theta} + k_{p_\theta}k_{d_x}\right)\right] = 0 \tag{4.36}$$

By solving (4.35) and (4.36) for the control gains k_{p_x} and k_{d_x}, the in (4.22) and (4.23) are

obtained. Moreover, the root s_{0_x} reaches a multiplicity 4 if and only if:

$$\Delta_x''(s_{0_x}) = 2\left(6s_{0_x}^2 + 3k_{d_\theta}s_{0_x} + k_{p_\theta}\right) +$$
$$e^{-\tau s_{0_x}}\left\{\tau^2\left(k_{d_x}s_{0_x} + k_{p_x}\right)\left(k_{d_\theta}s_{0_x} + k_{p_\theta}\right) - 2\tau\left(2k_{d_\theta}k_{d_x}s_{0_x} + k_{p_x}k_{d_\theta} + k_{p_\theta}k_{d_x}\right)\right.$$
$$\left. +2k_{d_x}k_{d_\theta}\right\} = 0 \tag{4.37}$$
$$\Delta_x'''(s_{0_x}) = 6\left(4s_{0_x} + k_{d_\theta}\right) -$$
$$e^{-\tau s_{0_x}}\left\{\tau^3\left(k_{d_x}s_{0_x} + k_{p_x}\right)\left(k_{d_\theta}s_{0_x} + k_{p_\theta}\right) + 3\tau^2\left(2k_{d_\theta}k_{d_x}s_{0_x} + k_{p_x}k_{d_\theta} + k_{p_\theta}k_{d_x}\right)\right.$$
$$\left. -6\tau k_{d_x}k_{d_\theta}\right\} = 0 \tag{4.38}$$

The substitution of (4.22) and (4.23) into the equations above, and the use of the `CellDecomposition` routine from the `RootFinding[Parametric]` package of computer algebra system `Maple` [33], led to (4.21) yet, one must analyse with detail the results concerning the in (4.21) and (4.24). For these ends, let one adopt the change of variable $\varsigma = s_{0_x}\tau$ throughout (4.24)-(4.34) yielding to rewrite the expressions as follows:

$$p_3^\star\lambda^3 + p_2^\star\lambda^2 + p_1^\star\lambda + p_0^\star = 0 \tag{4.39}$$
$$p_3^\star = 27\left(\varsigma^2 + 4\varsigma + 2\right)^4 \tag{4.40}$$
$$p_2^\star = -10\varsigma^9 - 243\varsigma^8 - 2352\varsigma^7 - 12090\varsigma^6 - 36360\varsigma^5 - 65916\varsigma^4 - 72288\varsigma^3 - 47736\varsigma^2$$
$$-17280\varsigma - 2592 \tag{4.41}$$
$$p_1^\star = \left(\varsigma^3 + 12\varsigma^2 + 36\varsigma + 24\right)\left(\varsigma^3 + 18\varsigma^2 + 54\varsigma + 24\right)\left(\varsigma^4 + 8\varsigma^3 + 24\varsigma^2 + 24\varsigma + 12\right) \tag{4.42}$$
$$p_0^\star = -\left(\varsigma^4 + 8\varsigma^3 + 24\varsigma^2 + 24\varsigma + 12\right)\left(\varsigma^3 + 12\varsigma^2 + 36\varsigma + 24\right)^2 \tag{4.43}$$
$$n_2^\star = 11\varsigma^{12} + 309\varsigma^{11} + 3738\varsigma^{10} + 25938\varsigma^9 + 115452\varsigma^8 + 348192\varsigma^7 + 731016\varsigma^6 + 1077408\varsigma^5$$
$$+1105920\varsigma^4 + 771120\varsigma^3 + 347328\varsigma^2 + 90720\varsigma + 10368 \tag{4.44}$$
$$n_1^\star = \left(\varsigma^3 + 12\varsigma^2 + 36\varsigma + 24\right)\left(2\varsigma^6 + 39\varsigma^5 + 249\varsigma^4 + 744\varsigma^3 + 1116\varsigma^2 + 756\varsigma + 180\right)$$
$$\left(\varsigma^4 + 8\varsigma^3 + 24\varsigma^2 + 24\varsigma + 12\right) \tag{4.45}$$
$$n_0^\star = 2\left(\varsigma^3 + 6\varsigma^2 + 12\varsigma + 6\right)\left(\varsigma^4 + 8\varsigma^3 + 24\varsigma^2 + 24\varsigma + 12\right)\left(\varsigma^3 + 12\varsigma^2 + 36\varsigma + 24\right)^2 \tag{4.46}$$
$$d_2^\star = 3\left(2\varsigma^3 + 9\varsigma^2 + 12\varsigma + 6\right)\left(\varsigma^2 + 4\varsigma + 2\right)^4 \tag{4.47}$$
$$d_1^\star = (\varsigma^4 + 16\varsigma^3 + 63\varsigma^2 + 84\varsigma + 30)(\varsigma^4 + 8\varsigma^3 + 24\varsigma^2 + 24\varsigma + 12)(\varsigma^2 + 4\varsigma + 2)^2 \tag{4.48}$$
$$d_0^\star = (\varsigma + 2)\left(\varsigma^3 + 12\varsigma^2 + 36\varsigma + 24\right)\left(\varsigma^4 + 8\varsigma^3 + 24\varsigma^2 + 24\varsigma + 12\right)\left(\varsigma^2 + 4\varsigma + 2\right)^2 \tag{4.49}$$

As previously mentioned, to exploit the results of [4, 12], the non-delayed part of the quasipolynomial must have only real roots which is guaranteed if (4.19) holds, thus it follows that $\lambda > 0$ as $s_{0_x}^2 > 0$ and, from (4.39)-(4.49), that

$$\frac{n_2^\star\lambda^2 - n_1^\star\lambda + n_0^\star}{d_2^\star\lambda^2 - d_1^\star\lambda + d_0^\star} > 18\sqrt{\lambda} \tag{4.50}$$

To ensure the existence of a given λ satisfying the condition above, some restrictions over ς (consequently over τ and s_{0_x}) must be established. In this regard, the analysis of the polynomial in (4.39) can be performed in any mathematical software that allows the treatment of symbolic and numerical computations. In the current case of study, Maple and its package *RootFinding[Parametric]* were used.

The aforementioned Maple package divides the space of parameters into two parts: the discriminant variety and its complement. The discriminant variety is referred as a generalization of the discriminant of a univariate polynomial and contains those parameter values leading to non-generic solutions, meanwhile, its complement can be expressed as a finite union of open cells such that the number of real solutions of the system is constant on each cell. In this manner, all parameter values leading to generic solutions of the system can be described. The underlying techniques used are Gröbner bases, polynomial real root finding, and cylindrical algebraic decomposition, see for instance [32, 34, 47, 49]. Further details of the package and its implementation are available at [24, 37]. Thus, considering (4.50) and the fact that $\lambda > 0$, the cell decomposition of (4.39) provides three ς intervals where the conditions holds. These intervals are defined by the projection polynomials:

$$\varphi_1(\varsigma) = \varsigma^{12} - 78\varsigma^{10} - 120\varsigma^9 + 2772\varsigma^8 + 13824\varsigma^7 + 8208\varsigma^6 - 105408\varsigma^5 - 357696\varsigma^4 - 546048\varsigma^3 - 456192\varsigma^2 - 207360\varsigma - 41472 \tag{4.51}$$

$$\varphi_2(\varsigma) = \varsigma^2 + 4\varsigma + 2, \quad \varphi_3(\varsigma) = \varsigma^3 + 9\varsigma^2 + 18\varsigma + 6 \tag{4.52}$$

and their real roots, such that

$$\varsigma_{\varphi_1,1} \approx -0.8478574488 < \varsigma < \varsigma_{\varphi_2,2} \approx -0.5857864376 \tag{4.53}$$

$$\varsigma_{\varphi_2,2} \approx -0.5857864376 < \varsigma < \varsigma_{\varphi_3,3} \approx -0.4157745568 \tag{4.54}$$

$$\varsigma_{\varphi_3,3} \approx -0.4157745568 < \varsigma < 0 \tag{4.55}$$

where $\varsigma_{\varphi_i,j}$ denotes the $j-th$ real root of the projection polynomial $\varphi_i(\varsigma)$ (considering that the real roots are arranged in increasing order). For instance, only the conditions over ς that ensure the existence of a proper λ have been given thus, one shall investigate the dominancy of the corresponding roots within the intervals.
As suggested in [4, 5, 9], if the quasipolynomial in (4.10) possesses a root of multiplicity at least 4, an integral representation can be adopted. The computation of the control gains as previously performed, allows one to establish a negative real root of multiplicity 4 thus, the substitution of (4.21)-(4.23) into (4.10) yields to:

$$\Delta_x(s; s_{0_x}, \tau) = (s - s_{0_x})^4 \left(1 + \int_0^1 e^{-(s-s_{0_x})\tau\upsilon} \frac{\tau R_{3,x}(s_{0_x}; \tau\upsilon)}{3!} d\upsilon\right) \tag{4.56}$$

such that:

$$R_{3,x}(s_{0_x}; \tau\upsilon) = s_{0_x}\left[s_{0_x}^3\tau^3\upsilon^3\left(1 + \lambda - \frac{1}{9}\frac{n_2\lambda^2 - n_1\lambda + n_0}{d_2\lambda^2 - d_1\lambda + d_0}\right) + 6s_{0_x}^2\tau^2\upsilon^2\left(2 + \lambda - \frac{1}{6}\frac{n_2\lambda^2 - n_1\lambda + n_0}{d_2\lambda^2 - d_1\lambda + d_0}\right) + 6s_{0_x}\tau\upsilon\left(6 + \lambda - \frac{1}{3}\frac{n_2\lambda^2 - n_1\lambda + n_0}{d_2\lambda^2 - d_1\lambda + d_0}\right) + 2\left(12 - \frac{1}{3}\frac{n_2\lambda^2 - n_1\lambda + n_0}{d_2\lambda^2 - d_1\lambda + d_0}\right)\right] \tag{4.57}$$

The results in [12] provide a necessary and sufficient condition for the dominancy of a given multiple root (of maximal multiplicity) in the first-order case. The main idea of the cited work is used in the current case of study to get sufficient conditions for the dominancy of the quadruple root at s_{0_x}, such that if:

$$\left|\frac{\tau R_{3,x}(s_{0_x}; \tau\upsilon)}{3!}\right| \leq 1 \quad \forall\ 0 < \upsilon < 1 \tag{4.58}$$

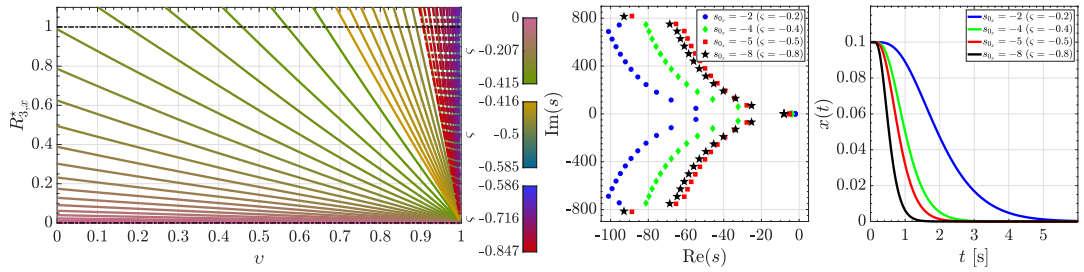

Figure 4.2: (left) Behavior of $R^{\star}_{3,x}(\varsigma;\upsilon)$ within the interval $0<\upsilon<1$. Numerical evidence of the dominancy of the root s_{0_x} within the intervals in (4.53)-(4.55) with $\tau=0.1$ [s]: (Center) Spectral distribution of the roots. (Right) Time-domain solution.

holds, s_{0_x} is the dominant root of (4.10). Nevertheless, to keep the consistency of the proof, one may rewrite (4.58) in terms of ς as follows:

$$\left|R^{\star}_{3,x}\left(\varsigma;\upsilon\right)\right|\leq 1 \quad \forall\ 0<\upsilon<1 \tag{4.59}$$

with

$$\begin{aligned}R^{\star}_{3,x}\left(\varsigma;\upsilon\right)=\frac{1}{6}\Bigg[&\varsigma^4\upsilon^3\left(1+\lambda-\frac{1}{9}\frac{n_2^{\star}\lambda^2-n_1^{\star}\lambda+n_0^{\star}}{d_2^{\star}\lambda^2-d_1^{\star}\lambda+d_0^{\star}}\right)+6\varsigma^3\upsilon^2\left(2+\lambda-\frac{1}{6}\frac{n_2^{\star}\lambda^2-n_1^{\star}\lambda+n_0^{\star}}{d_2^{\star}\lambda^2-d_1^{\star}\lambda+d_0^{\star}}\right)\\&+6\varsigma^2\upsilon\left(6+\lambda-\frac{1}{3}\frac{n_2^{\star}\lambda^2-n_1^{\star}\lambda+n_0^{\star}}{d_2^{\star}\lambda^2-d_1^{\star}\lambda+d_0^{\star}}\right)+2\varsigma\left(12-\frac{1}{3}\frac{n_2\lambda^2-n_1^{\star}\lambda+n_0^{\star}}{d_2^{\star}\lambda^2-d_1^{\star}\lambda+d_0^{\star}}\right)\Bigg]\end{aligned} \tag{4.60}$$

Due to the high order of the polynomials involved in the definition of $R^{\star}_{3,x}\left(\varsigma;\upsilon\right)$, an analytic analysis of its behavior results complex and computationally expensive, instead, a numerical analysis implies less computational resources and can provide enough and sufficient information to validate the proposal. In this regard, Fig. 4.2 exposes the plots of $R^{\star}_{3,x}\left(\varsigma;\upsilon\right)$ for a given ς within each of the intervals in (4.53)-(4.55) such that υ varies from 0 to 1 in order to verify (4.59).

The results depicted in Figs. 4.2 show that for a given ς within the intervals in (4.53) and (4.54), the condition in (4.59) does not hold. On the other hand, for a given ς within the interval in (4.55), one can obtain a bound over ς such that (4.59) holds. By solving $R^{\star}_{3,x}\left(\varsigma;\upsilon=0\right)=1$, one finds that the aforementioned condition is satisfied if $0>\varsigma>-0.3109805570$ which ends the proof.

□

Notice that the numerical study revealed that for any ς within the intervals in (4.53)-(4.55), the dominancy of s_{0_x} holds (as illustrated in Fig. 4.2) yet, the analytic extension of the proof implies a further and more complex analysis that comprehends the definition of more inequalities and conditions over the integral.

5 UAV Control: The Tilting-Rotors Case

The analysis of the quadrotor endowed with tilting-rotors takes into consideration the prescribed linearized conditions established in Section 4, additionally, the small-angle approximation is extended to the tilt angles of the rotors β,α, i.e. $C_{\beta}\approx 1$, $S_{\beta}\approx\beta$, $C_{\alpha}\approx 1$

and $S_\alpha \approx \alpha$. In this regard, the dynamic model in (3.1), (3.2), (3.6) and (3.8) is linearized such that the corresponding representation in the frequency domains reads as:

$$\begin{cases} X(s) = \dfrac{1}{m_r s^2}\left(\left(F_{p_1}(s) + F_{p_3}(s)\right)\beta(s)\right), \quad Y(s) = \dfrac{1}{m_r s^2}\left(-\left(F_{p_2}(s) + F_{p_4}(s)\right)\alpha(s)\right) \\ Z(s) = \dfrac{1}{m_r s^2}\left(T(s) - m_r g\right), \quad \psi(s) = \dfrac{1}{I_z s^2}\tau_\psi(s), \quad \phi(s) = \dfrac{1}{I_x s^2}\left(\tau_\phi(s) + \rho_\phi(s)\right), \\ \qquad \theta(s) = \dfrac{1}{I_y s^2}\left(\tau_\theta(s) + \rho_\theta(s)\right) \end{cases} \tag{5.1}$$

It has been assumed that the rotational dynamics is faster than that of translation such that for a large enough time, $\phi(s)T(s),\ \theta(s)T(s) \to 0$ since $\phi(s), \theta(s), \psi(s) \to 0$. Additionally, the influence of the free-moments $\varepsilon\left(F_{p_1}(s) + F_{p_3}(s)\right)\beta(s)$ and $-\varepsilon\left(F_{p_2}(s) + F_{p_4}(s)\right)\alpha(s)$ is considered as a disturbance and denoted instead as $\rho_\phi(s)$ and $\rho_\theta(s)$, respectively. In addition, it can be appreciated that the 6 DOFs of the current quadrotor vehicle are decoupled which permits a separate treatment. Additionally, the linearization holds if the vehicle operates at $\phi, \theta, \psi \approx 0$ thus, the attitude controllers must keep the vehicle at such operational point.

As in Section 4, the $Z(s)$ and $\psi(s)$ dynamics is addressed firstly as they provide valuable information used in the sequel of the procedure. Thus, let $T(s)$ and $\tau_\psi(s)$ be used as the respective control inputs for $Z(s)$ and $\psi(s)$ in (5.1). Regarding the $\phi(s)$ and $\theta(s)$ motions of the vehicle, the corresponding control inputs $\tau_\phi(s)$ and $\tau_\theta(s)$ are defined as

$$\tau_\phi(s) = I_x \mathcal{C}^*_\phi(s) E_\phi(s) \quad \text{and} \quad \tau_\theta(s) = I_y \mathcal{C}^*_\theta(s) E_\theta(s) \tag{5.2}$$

where

$$\mathcal{C}^*_\phi(s) = k_{d_\phi} s + k_{p_\phi} + \frac{k_{i_\phi}}{s} \quad \text{and} \quad \mathcal{C}^*_\theta(s) = k_{d_\theta} s + k_{p_\theta} + \frac{k_{i_\theta}}{s} \tag{5.3}$$

correspond to linear PID controllers with gains $k_{p_\phi}, k_{p_\theta}, k_{d_\phi}, k_{d_\theta}, k_{i_\phi}, k_{i_\theta} > 0$ since the presence of disturbances could be neutralized by the effects of the integral term. These controllers can be tuned by means of spectral methods.

As in Section 4, it is assumed that $\tau_\psi(s) \to 0$ and $T(s) \to T_c = m_r g$ thus, from the in (3.5) and (3.7), $F_{p_1}(s) + F_{p_3}(s) \to T_c/2$ and $F_{p_2}(s) + F_{p_4}(s) \to T_c/2$. The latter is translated to (5.1) as follows:

$$X(s) = \frac{T_c}{2m_r s^2}\beta(s) \quad \text{and} \quad Y(s) = -\frac{T_c}{2m_r s^2}\alpha(s) \tag{5.4}$$

These assumptions lead to define $\alpha(s)$ and $\beta(s)$ as the control inputs that drive the translational states of the system such that:

$$\alpha(s) = -\frac{2m_r}{T_c}\mathcal{C}_y(s)E_y(s) \quad \text{and} \quad \beta(s) = \frac{2m_r}{T_c}\mathcal{C}_x(s)E_x(s) \tag{5.5}$$

with $\mathcal{C}_x(s)$, $\mathcal{C}_y(s)$, $E_x(s)$ and $E_y(s)$ being linear PD controllers and the error signals as in (4.6)-(4.7).

The dynamics of the servomotors are neglected since, according to the results reported in the literature (see for instance [1, 23, 51, 52]), it is relatively faster than that of the overall aircraft. Thus, the $\alpha(s)$ and $\beta(s)$ angles are assumed to be instantaneously tracked.

Lastly, the $X(s)$ and $\theta(s)$ closed-loop dynamics of the quadrotor with tilting-rotors is

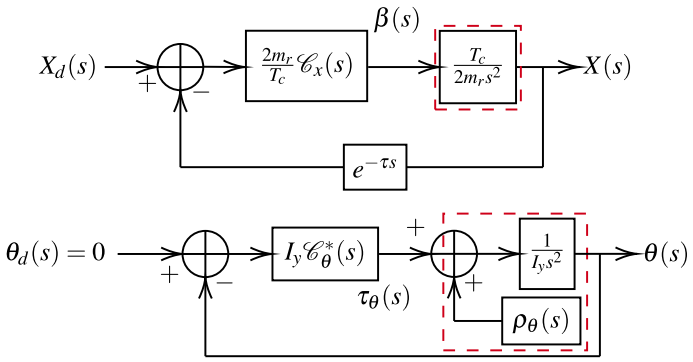

Figure 5.1: Block diagram representation of the quadrotor with tilting-rotors closed-loop system

depicted as block diagrams in Fig. 5.1. The diagram blocks regarding the $Z(s)$ and $\psi(s)$ dynamics coincide with those of the typical quadrotor vehicle shown in Fig. 4.1.

From Fig. 5.1, and recalling that the effect of the time-delay τ affects only the translational motion, one can find that the characteristic quasipolynomials of the concerned degrees of freedom are:

$$\Delta_x(s:k_{p_x},k_{d_x},\tau)=s^2+e^{-\tau s}\mathcal{C}_x(s),\quad \Delta_y(s:k_{p_y},k_{d_y},\tau)=s^2+e^{-\tau s}\mathcal{C}_y(s),$$
$$\Delta_z(s:k_{p_z},k_{d_z},\tau)=s^2+e^{-\tau s}\mathcal{C}_z(s) \tag{5.6}$$

Since the three characteristic quasipolynomials above have the form of that in (4.12), Proposition 4.2 is used to tune the controllers' gains.

6 Simulation Results

The actual section provides the results validating the proposed control scheme and tuning criteria. In this regard, a set of detailed numerical simulations, including the full nonlinear dynamics and the linearized one, was conducted. The parameters of the vehicles are listed in Table 1a meanwhile, the translational references to be achieved and tracked can be found as:

$$x_d(t)=\begin{cases}0 & 0\le t<20\\ \frac{20-t}{10} & 20<t<30\\ \frac{t-30}{5}-1 & 30<t<40\\ 1-\frac{t-40}{10} & 40<t<50\\ 0 & 50<t\le 70\end{cases}\qquad y_d(t)=\begin{cases}0 & 0\le t<10\\ 1 & 10<t<20\\ 1-\frac{t-20}{5} & 20<t<30\\ -1 & 30<t<40\\ \frac{t-40}{5}-1 & 40<t<50\\ 0 & 50<t\le 70\end{cases}$$

$$z_d(t)=\begin{cases}2 & 0\le t<30\\ 2-\frac{t-30}{10} & 30<t<40\\ 1 & 40<t<60\\ 0 & 60<t\le 70\end{cases} \tag{6.1}$$

where $x_d(t)$, $y_d(t)$ and $z_d(t)$ (given in [m]) denote the corresponding references and $t\ge 0$ stands for the time (in seconds [s]).

The study was conducted within the MATLAB/Simulink® 2018b environment, running

on an equipment with an 8GB RAM and an Inter® Core™ i5-8250 CPU @ 1.60 GHz & 1.80 GHz processor. Finally, the simulations took into consideration a time-delay τ of 0.1 [s]. Further details concerning the controllers' gains and the behavior of each system are provided in the upcoming subsections.

6.1 Simulation results: The Typical Quadrotor Case

With base on Proposition 4.2, the controller of the altitude (z) was tuned. The rightmost root was found to be $s_{0_z} \approx -5.85786437$. On the other hand, for the x and y controllers, Proposition 4.3 was used such that $s_{0_x} = s_{0_y} = -2$. The results of the tuning criteria led to the control gains summarized in Table 1b where the gains denoted by a $\star$ where computed (for comparison purposes) with base on the results at [19] such that it was considered that $\sigma_{x,y,z} = s_{0_{x,y,z}}$ to apply the σ-stability criteria. In this matter, it is worth highlighting that with the given control gains $s_{\phi,1} = s_{\theta,1} \approx -9.515844632$ and $s_{\phi,2} = s_{\theta,2} \approx -1.135739338$ such that $s_{\theta,1} < s_{0_x} < s_{\theta,2}$ (respectively $s_{\phi,1} < s_{0_y} < s_{\phi,2}$) thus, the overall dynamics of the system can be considered to be slightly faster than that of the inner loop but still bounded. The results of the numerical simulation depicted throughout Fig. 6.1 suggest that such difference is acceptable since the UAV achieves and successfully tracks the desired references.
In Fig. 6.1, the left-column results correspond to the vehicle's translational motion, while

Table 1: Definition of the vehicle's parameters and control gains

(a) Parameters of the UAVs

Parameter	**Nominal value**
m_r	0.675 kg
I_x, I_y	0.271 kg m^2
I_z	0.133 kg m^2
ℓ	0.45 m
g	9.81 m/s^2
ε	0.34 m

(b) Control gains: Typical quadrotor

DOF	k_p	k_d
x, y	1.658539	1.842677
z	7.91223	4.611587
ϕ, θ	10.80751	10.65158
ψ	10	15
* x, y	2.8	2.15
* z	8.1	3.64

(c) Control gains: Quadrotor endowed with titling rotors

DOF	k_p	k_d	k_i
x, y, z	7.91223	4.611587	
ϕ, θ	10	15	0.5
ψ	10	15	
* x, y, z	8.1	3.64	

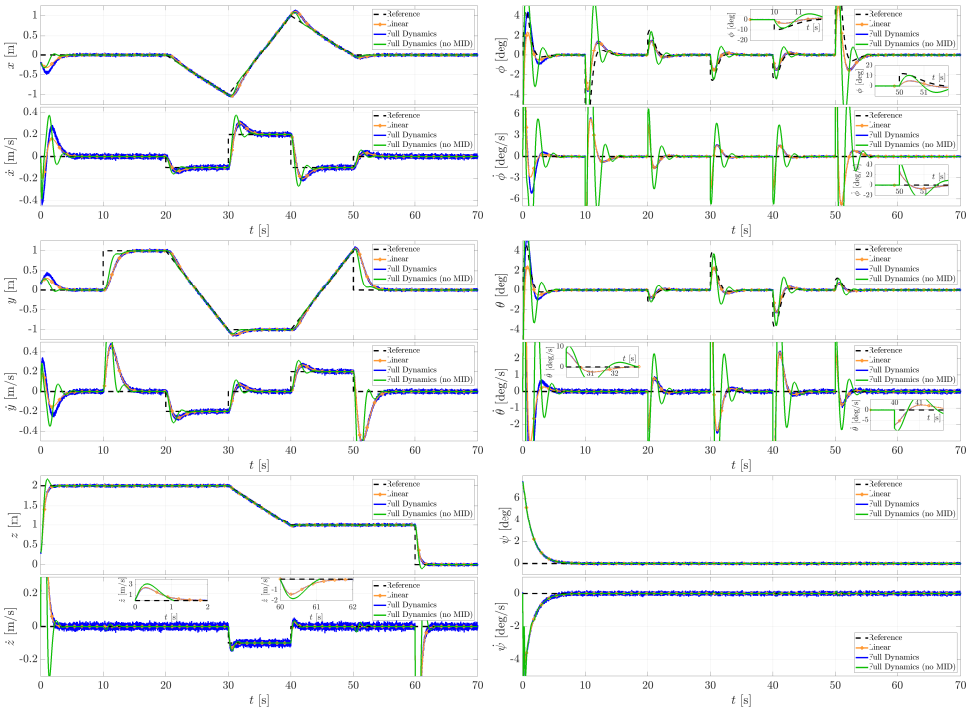

Figure 6.1: Motion of the typical quadrotor vehicle: Left) Translational states. Right) Rotational states.

the right-column plots exhibit the UAV's rotational behavior. In this regard, the black signals stand for the reference values, the black noisy signals correspond to the response of the non-linear system and the orange lines describe the behavior of the linearized system. The signals in green depict the behavior of the vehicle whose controllers were tuned with base on the results of [19].

As it can be appreciated in Fig. 6.1, the vehicle reaches the desired translational references, moreover, the performance of the non-linear system matches that of the vehicle whose dynamics is provided by the linear model. Nevertheless, one may pay special attention to the z motion as the behavior of the vehicle differs; in this sense, the vehicle with non-linear dynamics experiences some disturbances related to the real couplings existing due to the inherent nature of the UAV, however, the vehicle converges to the reference value in a relatively short time. Regarding the rotational motion of the quadrotor, depicted in Fig. 6.1, it comes to be evident to relate the corresponding peaks on the signals to the corresponding translation DOFs at which they are coupled, such that a change in the desired orientation occurs as the translational desired behavior changes.
In comparison with previous results (see for instance [19, 39, 44, 55, 58, 61]) and the ones depicted in green in Fig. 6.1, the vehicle operates with no overshoot or oscillation during the transient phase. The latter occurs as the real part of the dominant roots, for the case depicted in green, is lesser than the corresponding σ yet, these roots have an imaginary component since it is impossible, by the approach in [19], to know the exact location of the dominant roots meanwhile, the MID tuning criteria proposed in this work allows one to place the dominant roots exactly over the real axis. A similar behavior can be appreciated in the response of the quadrotor with tilting rotors.

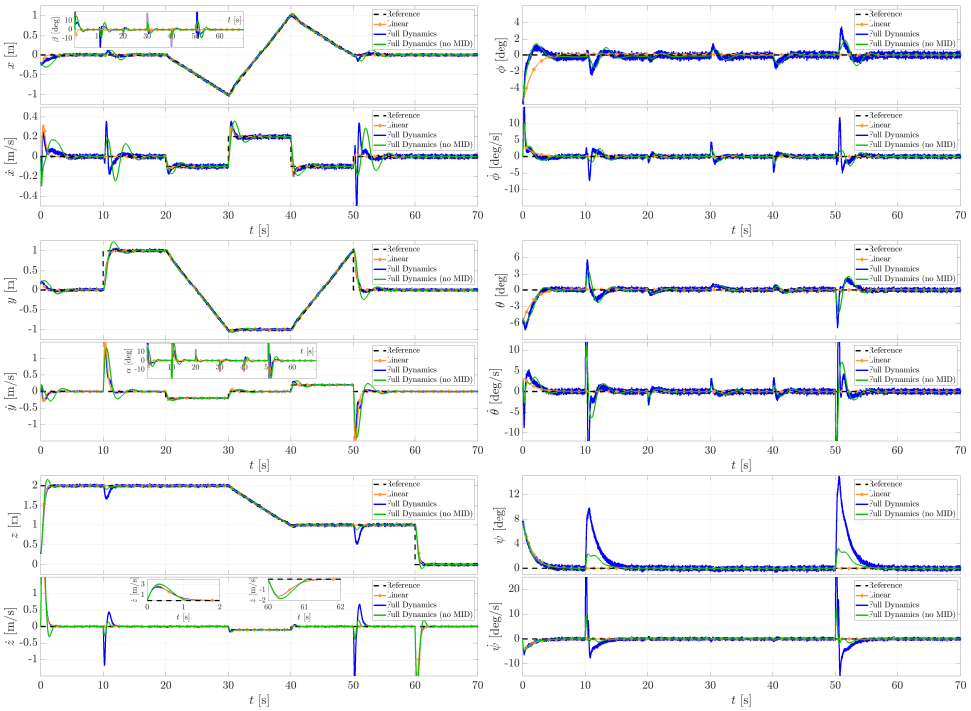

Figure 6.2: Motion of the quadrotor vehicle endowed with tilting-rotors: Left) Translational states. Right) Rotational states.

6.2 Simulation results: The Tilting-Rotors Case

As discussed in Section 5, to tune the controllers regarding this quadrotor, Proposition 4.2 was used thus, the control gains in Table 1c were found. The results of the simulation are depicted throughout Fig. 6.2 such that the translational motion is described by the plots at the left, and the plots at the right column depict the rotational states of the corresponding vehicle. The response of the servomotors is also depicted in the corresponding figures.

In comparison with the typical quadrotor vehicle, the translational states of the system seem to follow a similar behavior than that previously obtained, nevertheless, Fig. 6.2 shows the existence of a coupling between the three DOFs, in this sense, one may recall the considerations assumed during the linearization and controllers conception such that the couplings are related to the tilting-rotors and the rotational dynamics.
Regarding the rotational motion of the system, depicted in Fig. 6.2, it can be appreciated that the states of the system remain near to 0 [deg] as the servomotors' action permits to decouple the rotational and translational motions, at some point and under specific constrains. Nonetheless, the yaw angle seems to present a large deviation from the desired value due to the influence of the servomotors actuation which was neglected during the conception of the controllers yet, the orientation tends to be stabilized with no considerable consequence.

7 Concluding Remarks and Future Work

In this manuscript, the MID property has been exploited to tune stabilizing controllers of two representative aerial robotic systems. It has been shown by detailed numerical simulations that, by means of the MID property, the effects of the time-delayed feedback

that degrade the translational's motion of the vehicles can be mitigated since a proper assignment of the rightmost root of the characteristic function can be performed. As a consequence, the system's convergence rate is guaranteed to follow a prescribed behavior such that a fast non-oscillatory response is appreciated. Specific conditions and their corresponding proofs were introduced and detailed, leading to the control gains with respect to the time-delay value. The latter could equally serve as a tuning methodology proposal whether a time-delay can be induced in the feedback loop. Nonetheless, the experimental validation of the approach remains as a part of the upcoming work.
To the best of the authors' knowledge, a similar analytical and/or symbolic/numerical method to accurately determine the gains of the controllers for quadrotors, under the conditions herein considered, is not available in current related literature.

References

[1] Ismail Al-Ali, Yahya Zweiri, Nawaf AMoosa, Tarek Taha, Jorge Dias, and Lakmal Senevirtane. State of the art in tilt-quadrotors, modelling, control and fault recovery. *Proceedings of the Institution of Mechanical Engineers, Part C: Journal of Mechanical Engineering Science*, 234(2):474–486, 2020.

[2] J Alvarez-Munoz, Nicolas Marchand, JF Guerrero-Castellanos, JJ Tellez-Guzman, J Escareno, and Micky Rakotondrabe. Rotorcraft with a 3dof rigid manipulator: quaternion-based modeling and real-time control tolerant to multi-body couplings. *International Journal of Automation and Computing*, 15(5):547–558, 2018.

[3] JU Alvarez-Muñoz, JJ Castillo-Zamora, J Escareno, Islam Boussaada, F Mendez-Barrios, and O Labbani-Igbida. Time-delay control of a multi-rotor vtol multi-agent system towards transport operations. In *2019 International Conference on Unmanned Aircraft Systems (ICUAS)*, pages 276–283. IEEE, 2019.

[4] Tamas Balogh, Islam Boussaada, Tamas Insperger, and Silviu-Iulian Niculescu. Conditions for stabilizability of time-delay systems with real-rooted plant. *International Journal of Robust and Nonlinear Control*, pages 1–19, 2021.

[5] Tamas Balogh, Tamás Insperger, Islam Boussaada, and Silviu-Iulian Niculescu. Towards an mid-based delayed design for arbitrary-order dynamical systems with a mechanical application. In *21st IFAC World Congress*, pages 4375–4380, 2020.

[6] Amina Benarab, Islam Boussaada, Karim Trabelsi, Guilherme Mazanti, and Catherine Bonnet. The mid property for a second-order neutral time-delay differential equation. In *2020 24th International Conference on System Theory, Control and Computing (ICSTCC)*, pages 7–12. IEEE, 2020.

[7] Islam Boussaada, Guilherme Mazanti, Silviu-Iulian Niculescu, Julien Huynh, Franck Sim, and Matthieu Thomas. Partial pole placement via delay action: A python software for delayed feedback stabilizing design. In *2020 24th International Conference on System Theory, Control and Computing (ICSTCC)*, pages 196–201. IEEE, 2020.

[8] Islam Boussaada and Silviu-Iulian Niculescu. Tracking the algebraic multiplicity of crossing imaginary roots for generic quasipolynomials: A vandermonde-based approach. *IEEE Transactions on Automatic Control*, 61(6):1601–1606, 2015.

[9] Islam Boussaada and Silviu-Iulian Niculescu. Characterizing the codimension of zero singularities for time-delay systems. *Acta Applicandae Mathematicae*, 145(1):47–88, 2016.

[10] Islam Boussaada, Silviu-Iulian Niculescu, Ali El Ati, Redamy Pérez-Ramos, and Karim Liviu Trabelsi. Multiplicity-induced-dominancy in parametric second-order delay differential equations: Analysis and application in control design. *ESAIM: Control, Optimisation and Calculus of Variations*, 2019.

[11] Islam Boussaada, Sami Tliba, Silviu-Iulian Niculescu, Hakki Ulaş Ünal, and Tomáš Vyhlídal. Further remarks on the effect of multiple spectral values on the dynamics of time-delay systems. application to the control of a mechanical system. *Linear Algebra and its Applications*, 542:589–604, 2018.

[12] Islam Boussaada, Hakki Ulaş Unal, and Silviu-Iulian Niculescu. Multiplicity and stable varieties of time-delay systems: A missing link. In *22nd International Symposium on Mathematical Theory of Networks and Systems (MTNS)*, pages –, 2016.

[13] Tauã Cabreira, Lisane Brisolara, and Paulo R Ferreira. Survey on coverage path planning with unmanned aerial vehicles. *Drones*, 3(1):4, 2019.

[14] Xibin Cao, Peng Shi, Zhuoshi Li, and Ming Liu. Neural-network-based adaptive backstepping control with application to spacecraft attitude regulation. *IEEE transactions on neural networks and learning systems*, 29(9):4303–4313, 2017.

[15] Jose J Castillo-Zamora, Karla A Camarillo-Gomez, Gerardo I Perez-Soto, and Juvenal Rodriguez-Resendiz. Comparison of pd, pid and sliding-mode position controllers for v–tail quadcopter stability. *Ieee Access*, 6:38086–38096, 2018.

[16] José J Castillo-Zamora, Karla A Camarillo-Gómez, Gerardo I Pérez-Soto, Juvenal Rodríguez-Reséndiz, and Luis A Morales-Hernández. Mini-AUV Hydrodynamic Parameters Identification via CFD Simulations and Their Application on Control Performance Evaluation. *Sensors*, 21(3):820, 2021.

[17] Jose J Castillo-Zamora, J Escareno, Islam Boussaada, J Stephant, and O Labbani. Nonlinear control of a multilink aerial system and asekf-based disturbances compensation. *IEEE Transactions on Aerospace and Electronic Systems*, 57(2):907–918, 2021.

[18] Jose J Castillo-Zamora, Juan Escareño, J Alvarez, Joanny Stephant, and Islam Boussaada. Disturbances and coupling compensation for trajectory tracking of a multi-link aerial robot. In *2019 6th International Conference on Control, Decision and Information Technologies (CoDIT)*, pages 738–743. IEEE, 2019.

[19] Jose J. Castillo-Zamora, Jose E. Hernández-Díez, Islam Boussaada, Juan Escareno, and Jonatan U. Alvarez-Muñoz. A preliminary parametric analysis of pid delay-based controllers for quadrotor uavs. In *2021 International Conference on Unmanned Aircraft Systems (ICUAS)*, pages 28–37, 2021.

[20] Yadong Ding, Yaoyao Wang, and Bai Chen. A practical time-delay control scheme for aerial manipulators. *Proceedings of the Institution of Mechanical Engineers, Part I: Journal of Systems and Control Engineering*, 235(3):371–388, 2021.

[21] Juan Escareño, Jesus Castillo, Wafik Abassi, Gerardo Flores, and Karla Camarillo. Navigation strategy in-flight retrieving and transportation operations for a rotorcraft mav. In *2017 Workshop on Research, Education and Development of Unmanned Aerial Systems (RED-UAS)*, pages 7–12. IEEE, 2017.

[22] Thomas E Fortmann and Konrad L Hitz. *An introduction to linear control systems*. Crc Press, 1977.

[23] Matthew J Gerber and Tsu-Chin Tsao. Twisting and tilting rotors for high-efficiency, thrust-vectored quadrotors. *Journal of Mechanisms and Robotics*, 10(6), 2018.

[24] Jürgen Gerhard, David J Jeffrey, and Guillaume Moroz. A package for solving parametric polynomial systems. *ACM Communications in Computer Algebra*, 43(3/4):61–72, 2010.

[25] Keqin Gu, Jie Chen, and Vladimir L Kharitonov. *Stability of time-delay systems*. Springer Science & Business Media, 2003.

[26] Jack K Hale and Sjoerd M Verduyn Lunel. *Introduction to functional differential equations*, volume 99. Springer Science & Business Media, 2013.

[27] N. D. Hayes. Roots of the transcendental equation associated with a certain difference-differential equation. *Journal of the London Mathematical Society*, s1-25(3):226–232, 1950.

[28] Markus Hehn and Raffaello D'Andrea. A flying inverted pendulum. In *2011 IEEE International Conference on Robotics and Automation*, pages 763–770. IEEE, 2011.

[29] Ran Jiao, Wusheng Chou, Yongfeng Rong, and Mingjie Dong. Anti-disturbance attitude control for quadrotor unmanned aerial vehicle manipulator via fuzzy adaptive sigmoid generalized super-twisting sliding mode observer. *Journal of Vibration and Control*, 0(0):–, 2021.

[30] Yusuf Kartal, Kamesh Subbarao, Nicholas R Gans, Atilla Dogan, and Frank Lewis. Distributed backstepping based control of multiple uav formation flight subject to time delays. *IET Control Theory & Applications*, 14(12):1628–1638, 2020.

[31] Prasanna Kolar, Nicholas Gamez, and Mo Jamshidi. Impact of time delays on networked control of autonomous systems. In *Beyond Traditional Probabilistic Data Processing Techniques: Interval, Fuzzy etc. Methods and Their Applications*, pages 151–178. Springer, 2020.

[32] Daniel Lazard. Computing with parameterized varieties. In *Algebraic geometry and geometric modeling*, pages 53–69. Springer, 2006.

[33] Daniel Lazard and Fabrice Rouillier. Solving parametric polynomial systems. *Journal of Symbolic Computation*, 42(6):636 – 667, 2007.

[34] Daniel Lazard and Fabrice Rouillier. Solving parametric polynomial systems. *Journal of Symbolic Computation*, 42(6):636–667, 2007.

[35] Lixin Li, Meng Wang, Kaiyuan Xue, Qianqian Cheng, Dawei Wang, Wei Chen, Miao Pan, and Zhu Han. Delay optimization in multi-uav edge caching networks: A robust mean field game. *IEEE Transactions on Vehicular Technology*, 2020.

[36] Shuo Li, Na Duan, Zhizheng Xu, and Xiaoyang Liu. Tracking control of quadrotor uav with input delay. In *2020 39th Chinese Control Conference (CCC)*, pages 646–649. IEEE, 2020.

[37] Songxin Liang, Jürgen Gerhard, and D Jeffrey. A new maple package for solving parametric polynomial systems, 2007.

[38] Ming Liu, Lixian Zhang, Peng Shi, and Yuxin Zhao. Fault estimation sliding-mode observer with digital communication constraints. *IEEE Transactions on Automatic Control*, 63(10):3434–3441, 2018.

[39] J López-Herńandez, J Escareno, C-F Méndez-Barrios, O Labbani, V Ramírez-Rivera, J Coronado, and Hector Méndez-Azúa. A comparative stability analysis of underactuated versus fully-actuated rotorcrafts having time-delay feedback. In *2019 6th International Conference on Control, Decision and Information Technologies (CoDIT)*, pages 1640–1645. IEEE, 2019.

[40] Dan Ma, Islam Boussaada, Catherine Bonnet, Silviu-Iulian Niculescu, and Jie Chen. Multiplicity-induced-dominancy extended to neutral delay equations: Towards a systematic pid tuning based on rightmost root assignment. In *2020 American Control Conference (ACC)*, pages 1690–1695. IEEE, 2020.

[41] Guilherme Mazanti, Islam Boussaada, and Silviu-Iulian Niculescu. On qualitative properties of single-delay linear retarded differential equations: Characteristic roots of maximal multiplicity are necessarily dominant. *IFAC-PapersOnLine*, 53(2):4345–4350, 2020.

[42] Guilherme Mazanti, Islam Boussaada, and Silviu-Iulian Niculescu. Multiplicity-induced-dominancy for delay-differential equations of retarded type. *Journal of Differential Equations*, 286:84–118, 2021.

[43] Wim Michiels and Silviu-Iulian Niculescu. *Stability, control, and computation for time-delay systems: an eigenvalue-based approach*. SIAM, 2014.

[44] Omid Mofid, Saleh Mobayen, Chunwei Zhang, and Balasubramanian Esakki. Desired tracking of delayed quadrotor UAV under model uncertainty and wind disturbance using adaptive super-twisting terminal sliding mode control. *ISA transactions*, 2021.

[45] Csenge A Molnar, Tamas Balogh, Islam Boussaada, and Tamas Insperger. Calculation of the critical delay for the double inverted pendulum. *Journal of Vibration and Control*, page 1077546320926909, 2020.

[46] Jafet Morales, Gerson Rodriguez, Grant Huang, and David Akopian. Toward uav control via cellular networks: Delay profiles, delay modeling, and a case study within the 5-mile range. *IEEE Transactions on Aerospace and Electronic Systems*, 56(5):4132–4151, 2020.

[47] Guillaume Moroz. *Sur la décomposition réelle et algébrique des systemes dépendant de parametres*. PhD thesis, Université Pierre et Marie Curie-Paris VI, 2008.

[48] S-I Niculescu and Wim Michiels. Stabilizing a chain of integrators using multiple delays. *IEEE Transactions on Automatic Control*, 49(5):802–807, 2004.

[49] Fabrice Rouillier. Solving zero-dimensional systems through the rational univariate representation. *Applicable Algebra in Engineering, Communication and Computing*, 9(5):433–461, 1999.

[50] Fabio Ruggiero, Vincenzo Lippiello, and Anibal Ollero. Aerial manipulation: A literature review. *IEEE Robotics and Automation Letters*, 3(3):1957–1964, 2018.

[51] Markus Ryll, Heinrich H Bülthoff, and Paolo Robuffo Giordano. A novel overactuated quadrotor unmanned aerial vehicle: Modeling, control, and experimental validation. *IEEE Transactions on Control Systems Technology*, 23(2):540–556, 2014.

[52] Abdul-Wahid A Saif, Abdulrahman Aliyu, Mujahed Al Dhaifallah, and Moustafa Elshafei. Decentralized backstepping control of a quadrotor with tilted-rotor under wind gusts. *International Journal of Control, Automation and Systems*, 16(5):2458–2472, 2018.

[53] Joel L Schiff. *The Laplace transform: theory and applications*. Springer Science & Business Media, 1999.

[54] Hazim Shakhatreh, Ahmad H Sawalmeh, Ala Al-Fuqaha, Zuochao Dou, Eyad Almaita, Issa Khalil, Noor Shamsiah Othman, Abdallah Khreishah, and Mohsen Guizani. Unmanned aerial vehicles (uavs): A survey on civil applications and key research challenges. *IEEE Access*, 7:48572–48634, 2019.

[55] Manmohan Sharma and Indrani Kar. Control of a quadrotor with network induced time delay. *ISA transactions*, 111:132–143, 2021.

[56] Junpei Shirai, Takashi Yamaguchi, and Kiyotsugu Takaba. Remote visual servo tracking control of drone taking account of time delays. In *2017 56th Annual Conference of the Society of Instrument and Control Engineers of Japan (SICE)*, pages 1589–1594. IEEE, 2017.

[57] Rifat Sipahi, Silviu-Iulian Niculescu, Chaouki T Abdallah, Wim Michiels, and Keqin Gu. Stability and stabilization of systems with time delay. *IEEE Control Systems Magazine*, 31(1):38–65, 2011.

[58] Eduardo Steed, Espinoza Quesada, Luis Rodolfo, Garcia Carrillo, Adria N Ramirez, and Sabine Mondie. Algebraic dominant pole placement methodology for unmanned aircraft systems with time delay. *IEEE Transactions on Aerospace and Electronic Systems*, 52(3):1108–1119, 2016.

[59] Wei Wang, Kenzo Nonami, Mitsuo Hirata, and Osamu Miyazawa. Autonomous control of micro flying robot. *Journal of Vibration and Control*, 16(4):555–570, 2010.

[60] Shengyuan Xu and James Lam. A survey of linear matrix inequality techniques in stability analysis of delay systems. *International Journal of Systems Science*, 39(12):1095–1113, 2008.

[61] Zhen Xu, Mingchu Xu, Yifei Wu, Qingwei Chen, and Enze Zhang. Distributed hunting problem of multi-quadrotor systems via bearing constraint method subject to time delays. *Journal of the Franklin Institute*, 357(12):7537–7555, 2020.